JOURNAL OF THEORETICAL
AND APPLIED MECHANICS
https://doi.org/10.15632/jtam-pl/203595
ONLINE FIRST

EXPERIMENTAL STUDY ON MECHANICAL PROPERTIES OF RED SANDSTONE UNDER CYCLIC LOAD AFTER DRY-WET CYCLES

Hongjun LI[1], Baoyun ZHAO[2*], Liyun ZHANG[3], Hang ZOU[4]

[1] *China Anergy Group Third Engineering Bureau Co.Ltd., Chengdu 610036, China*
[2] *School of Civil and Hydraulic Engineering, Chongqing University of Science and Technology, Chongqing 401331, China*
[3] *Finance Bureau of Korla City, Bazhou 841000, Xinjiang, China*
[4] *Chongqing Industry Polytechnic College, Chongqing 401120, China*
*corresponding author, *baoyun666@cqust.edu.cn*

This study investigates the mechanical properties of red sandstone in the Three Gorges Reservoir area under cyclic loading after dry-wet cycles. Results show that the first five cycles significantly affect the dry mass, with a 1.16 % decrease. Under the same cyclic loads, peak stress decreases with increasing dry-wet cycles, and stress-strain curves exhibit hysteresis loops. Elastic modulus increases in stages with the stress amplitude, with the first five cycles having the most significant impact. These findings offer crucial theoretical guidance for safeguarding hazardous slopes within the drawdown zone of the Three Gorges Reservoir.

Keywords: dry-wet cycle; red sandstone; mechanical properties; cyclic loading.

1. Introduction

The bank's rock slopes have undergone varying intensities of dry-wet cycles resulting from periodic fluctuations in reservoir water levels (Liu *et al.*, 2022; Zhao *et al.*, 2017; Akcanca & Aytekin, 2014). The rock engineering of reservoir banks, such as bank slope roads and bridge foundations, is often affected by cyclic loads caused by vehicle vibrations. The rock slope engineering on the reservoir bank may be affected by dynamic loads, such as earthquakes and blasting, following the dry-wet cycle. Therefore, investigating the mechanical properties of rocks under cyclic loading after undergoing dry-wet cycles is of preeminent importance.

Repeated dry-wet cycles degrade the mechanical properties of rocks, resulting in deformation and eventual failure of the rock mass (Huang *et al.*, 2022). In the past few decades, extensive experimental studies have focused on examining how dry-wet cycles affect the weakening of different rock types (Huan *et al.*, 2024; Cao *et al.*, 2022; Wang *et al.*, 2023). Ma *et al.* (2022) found that the uniaxial compressive strength (UCS) of sandstone decreases by 4.58 % in a single dry-wet cycle and by 18.35 % after 20 cycles. Hu *et al.* (2022) observed a reduction in the quality, hardness, and surface gloss of coal samples, alongside an increase in surface roughness after 50 dry-wet cycles. Zheng *et al.* (2023) noted that the elastic modulus, cohesion, and friction of argillaceous sandstone significantly deteriorated during the initial dry-wet cycles, followed by a gradual decline after 10 cycles. Furthermore, utilizing the energy dissipation theory, Chen *et al.* (2019) discovered that rock energy dissipation progressively increased with the number of dry-wet cycles. The energy evolution of rock samples is categorized into the initial dissipation energy stage, stable dissipation energy growth stage, dissipation energy acceleration stage, and dissipation energy surge stage. Liu *et al.* (2019) based their research on thermodynamics and energy dissipation principles to formulate damage evolution equations for red sandstone subjected to various dry-wet cycles.

Since 2005, numerous researchers have conducted studies investigating the impact of cyclic loadings on the fatigue properties of rocks. A series of fatigue tests have been performed to examine fatigue and energy dissipation in materials such as sandstone (Zhao *et al.*, 2023; 2024), marble (Wang *et al.*, 2021), granite (Zhou *et al.*, 2021), and other materials (Zhou *et al.*, 2023). In the field of rock fatigue characteristics, factors such as loading frequency, temperature, stress amplitude, and cycle number have been identified as significantly impacting the strength of rock masses during cyclic loading and unloading tests. In the domain of energy dissipation, researchers utilize the internal elastic energy principle of rocks to analyze energy evolution trends under fatigue loading. Li *et al.* (2023) demonstrated that the total energy involved in the energy transformation process encompasses both elastic energy, representing elastic deformation, and dissipated energy, which accounts for anchor deformation, fracture propagation, and plastic damage. Gao *et al.* (2022) discovered that the elastic strain and elastic energy density increase linearly with deviatoric stress and are proportional to confining pressure and loading rate. Conversely, the irreversible strain and dissipated energy density increase exponentially with the deviatoric stress.

In summary, extensive research has been conducted on the effects of dry-wet cycles on the mechanical properties of rocks, as well as on the cyclic loading mechanical properties of rocks, yielding significant and valuable findings. This paper focuses on the rock slopes within the fluctuating zone of the Three Gorges Reservoir as the primary research subject. Considering the actual environmental conditions of the slope, this study explores the mechanical characteristics of red sandstone under cyclic loading following various numbers of dry-wet cycles. Cyclic loading tests were performed on representative red sandstone samples from the selected site, and a detailed analysis of energy dissipation in the sandstone samples was conducted.

2. Sample preparation and dry-wet cycle test

2.1. Red sandstone sample preparation

The samples were collected from the slope area with fluctuating water levels of the Three Gorges Reservoir in Chongqing, China (Chen *et al.*, 2023), which consisted of typical red sandstone. The test samples exhibited a dense structure with coarser mineral particles, a flesh-red color, and a density of approximately 2380 kg/m^3. Following the methodology proposed by the International Society for Rock Mechanics (ISRM) (Fairhurst & Hudson, 1999), all tested sandstone samples were cylindrical, with a diameter of approximately 50 mm and a length of 100 mm (see Fig. 1).

Fig. 1. Red sandstone samples.

2.2. Dry-wet cycle test

2.2.1. Testing procedure

To thoroughly investigate the effects of dry-wet cycles on the physical properties of red sandstone, five groups with varying numbers of dry-wet cycles were established (Zhao *et al.*, 2021), specifically 0, 10, 20, 30, and 40 cycles. The processed samples were initially dried in a dry-

ing oven at temperatures ranging from 105 °C to 110 °C for 12 hours. After a slight cooling to room temperature, the samples were subsequently placed in a vacuum saturation instrument for 12 hours to achieve saturation. This drying and saturation process was alternately repeated until the desired number of cycles was attained (see Fig. 2 for an illustration of the testing apparatus). Additionally, the samples were weighed after each drying and saturation cycle.

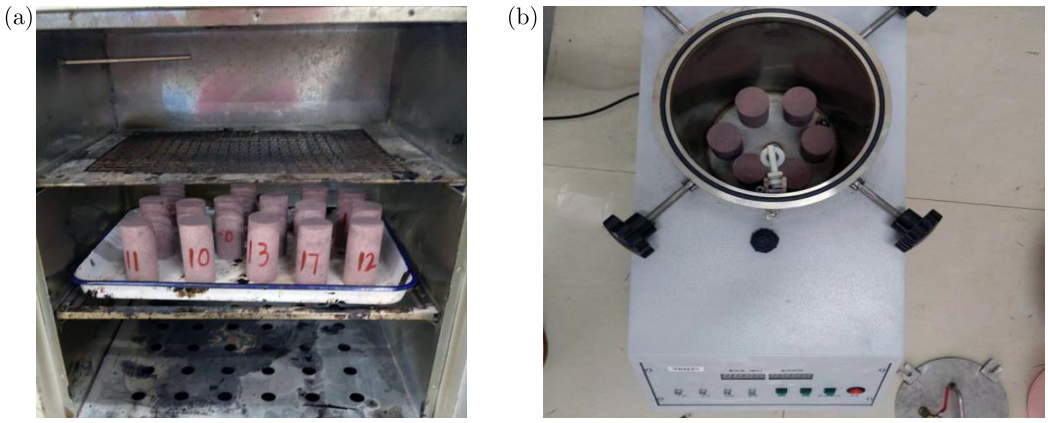

Fig. 2. Dry and wet cycle test apparatus: (a) drying box; (b) vacuum saturating instrument.

2.2.2. Change in law of dried and saturated mass

Figure 3 illustrates the mass of red sandstone after different dry and wet cycles. It can be observed that the curve of the dried mass no longer exhibits discernible changes after 5 cycles of the wet and dry decrease. It is important to note that the mass of the dried sample without a dry-wet cycle was 453.70 g. After 5 cycles, it decreased to 448.40 g, representing a decrease of 1.16 % compared to the initial mass. Subsequently, the mass of the dried sample showed no significant change. Conversely, the curve of the saturated mass increased rapidly after 5 dry and wet cycles and then reached a relatively steady state. Figure 3 illustrates that the initial 5 dry-wet cycles had a significant impact on the mass of sandstone.

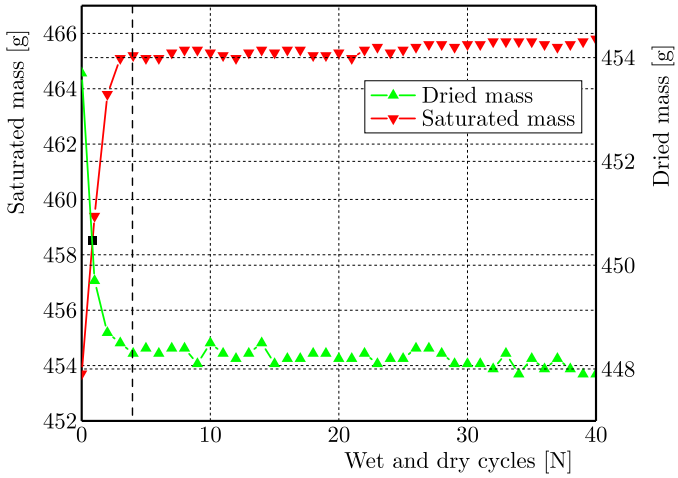

Fig. 3. Mass change of red sandstone under dry-wet cycle.

3. Cyclic loading and unloading tests on red sandstone after dry-wet cycles

3.1. Method of cyclic loading and unloading test

Building upon previous findings regarding the behavior of dried and saturated mass, this study employed red sandstone samples subjected to 0, 5, and 10 dry-wet cycles to perform uni-

axial cyclic loading and unloading tests. The lower limit of cyclic load stress was set at 5 MPa, while the upper limits were 10 MPa, 15 MPa, 20 MPa, 25 MPa, 30 MPa, 40 MPa, and 45 MPa, respectively. In other words, the stress amplitudes were 5 MPa, 10 MPa, 15 MPa, 20 MPa, 25 MPa, 30 MPa, 35 MPa, and 40 MPa, respectively. The loading frequency was 0.02 Hz and there were 10 loading and unloading cycles under the same stress amplitude. Upon completion of the loading and unloading cycles, a loading rate of 0.05 mm/min was applied continuously until the sample failure occurred. The detailed loading and unloading procedure is illustrated in Fig. 4.

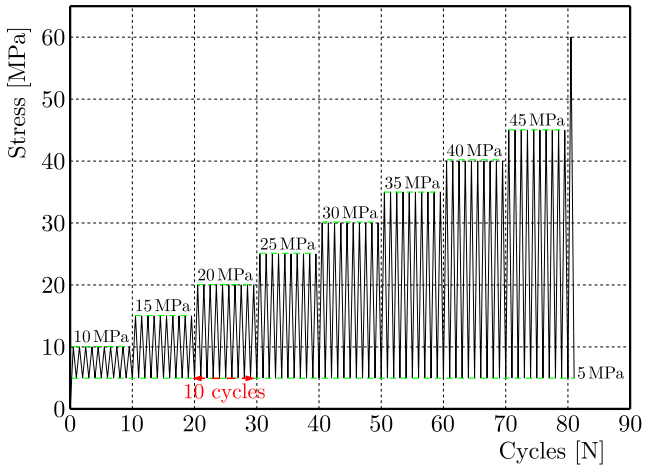

Fig. 4. Diagram of cyclic loading and unloading modes.

3.2. Testing equipment

The TFD-2000 microcomputer servo-controlled rock triaxial testing machine is utilized in the test, as shown in Fig. 5 (Li *et al.*, 2024). This equipment serves as the primary testing apparatus for evaluating the mechanical properties of materials such as rock and cement. It can be employed in various tests, including rock uniaxial compression test, triaxial compression test, and corresponding creep tests. The testing machine has a maximum axial compressive force of 2000 kN, with a force measurement error range of ±0.5 %. During testing, data on stress, strain, force, and displacement were automatically collected by microcomputers, recorded, and analyzed in real time.

Fig. 5. TFD-2000 microcomputer servo-controlled rock triaxial testing machine.

3.3. Stress-strain curve of red sandstone

Figure 6 illustrates the cyclic loading and unloading stress-strain curve of the red sandstone after undergoing dry-wet cycles. Under identical stress amplitudes, the hysteresis loops of the

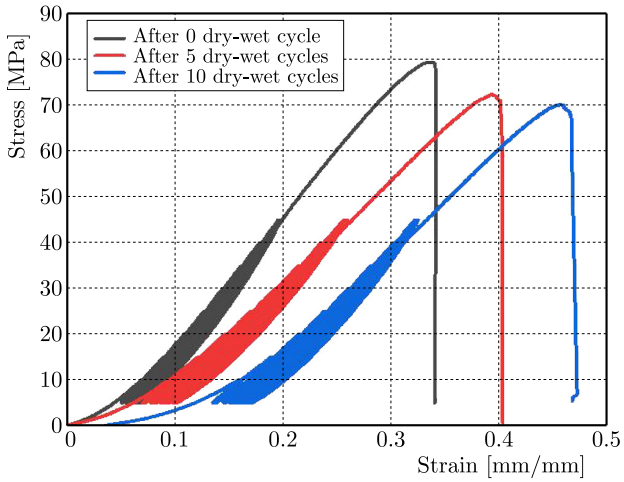

Fig. 6. Uniaxial stress-strain curves of red sandstone under different loading cycles after dry-wet cycles.

stress-strain curves for red sandstone samples exhibit a "sparse-to-dense" development pattern, with the area of the hysteresis loops gradually decreasing until reaching a stable state. Additionally, Fig. 6 shows that the slope of the stress-strain curve for red sandstone decreases as the number of dry-wet cycles increases, while the axial strain concurrently increases.

Figure 7 presents a comparison between the cyclic stress–strain curves of red sandstone and the uniaxial stress–strain curves of samples subjected to different dry-wet cycles. Figure 7 clearly demonstrates that the strength of red sandstone samples subjected to dry-wet cycles is significantly lower than that of samples without such cycles. The increases in lateral and axial strains due to dry-wet cycles can be attributed to the weakening of the rock strength caused by the accumulation of fatigue damage. As the stress amplitude increases, both lateral and axial strains of red sandstone also increase. Under identical stress conditions, axial strain is greater than lateral strain. The increase in axial strain is more pronounced at low stress amplitudes, whereas the opposite occurs at high stress amplitudes as the stress amplitude continues to rise.

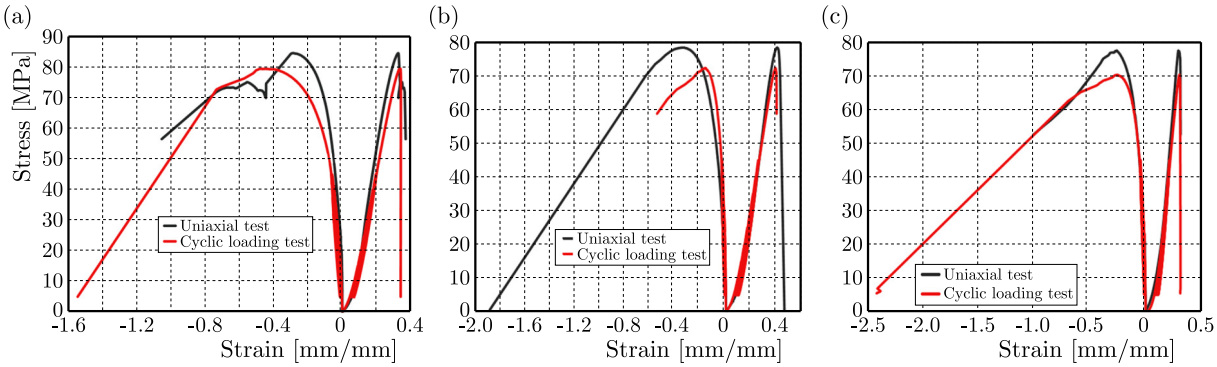

Fig. 7. Stress-strain curves of red sandstone under uniaxial cyclic loading after different dry-wet cycles: (a) 0 dry-wet cycle; (b) 5 dry-wet cycles; (c) 10 dry-wet cycles.

Figure 8 illustrates the comparison of the peak stress during the loading cycle of specimens after various dry-wet cycles with their uniaxial compressive strength (UCS). It is evident that the peak strength of both samples types decreases with the number of dry-wet cycles, mirroring the decrease in UCS. The decreasing trend of the peak stress during cyclic loading and unloading is more pronounced compared to UCS. This phenomenon suggests that cyclic loading intensified the internal damage within the rock, leading to its deteriorated state. Figure 8 shows that the initial strength of red sandstone samples is 84.48 MPa without cyclic loading. After undergoing

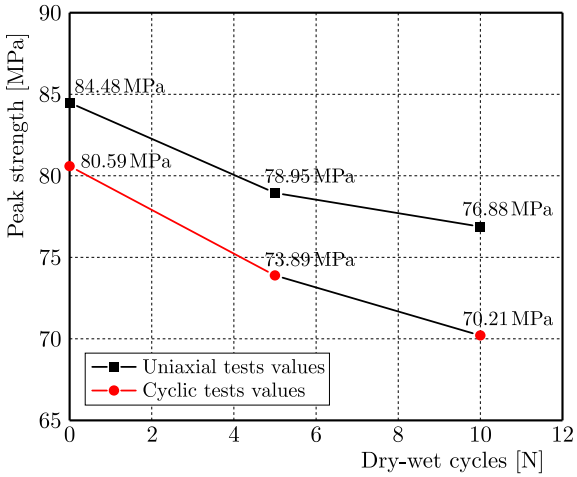

Fig. 8. Comparison of peak strength between conventional uniaxial results and uniaxial cyclic loading results.

5 dry-wet cycles, the strength decreases to 78.95 MPa, and further decreases to 76.88 MPa after 10 dry-wet cycles. Compared to the initial state, peak stress reductions were 6.55 % and 9.63 %, respectively. The peak stress of samples was significantly reduced under loading cycles of varying amplitudes, from 80.59 MPa after zero dry-wet cycles to 73.89 MPa after five cycles and further to 70.21 MPa after ten cycles. Compared to uniaxial strength under static loading conditions, the peak stress of red sandstone samples decreased by 4.60 %, 6.41 %, and 8.68 % after cyclic loading and unloading. According to statistical results, peak stress decreases with an increasing number of dry-wet cycles, with the most significant reduction occurring within the first 5 cycles.

3.4. Law of elastic modulus change

The elastic modulus is a critical parameter for evaluating the mechanical properties of rock. According to the "Regulation for Testing the Physical and Mechanical Properties of Rock – Part 19: Test for Determining the Deformability of Rock in Uniaxial Compression" (DZ/T 0276.19-2015), the elastic modulus for each load cycle is calculated using Eq. (3.1):

$$E = \frac{\sigma_{\max} - \sigma_{\min}}{\varepsilon_{\max} - \varepsilon_{\min}}, \tag{3.1}$$

where E is the elastic modulus (in MPa); $\sigma_{\max}$ is the maximum axial stress in each cycle (in MPa); $\sigma_{\min}$ is the minimum axial stress in each cycle; $\varepsilon_{\max}$ is the maximum axial strain, and $\varepsilon_{\min}$ is the minimum axial strain, respectively.

Using Eq. (3.1), the elastic modulus of the sample under different stress amplitudes after various dry-wet cycles was calculated, as presented in Table 1.

Figure 9 shows the variation of the elastic modulus of the red sandstone during different loading and unloading cycles after different dry-wet cycles. It is evident that there is a gradual increase in the overall elastic modulus. At relatively small stress amplitudes, the elastic modulus of the samples fluctuates with an increasing number of loading cycles. When the stress amplitude increases to 5 MPa–20 MPa, the change in elastic modulus becomes less significant with an increasing number of cyclic loading cycles. Additionally, Fig. 9 shows that the modulus of elasticity of rock samples decreases after being subjected to varying degrees of dry-wet cycles. The elastic modulus decreased significantly after the first 5 cycles, with a smaller decrease from cycles 5 to 10 compared to the initial five cycles.

Figure 10 illustrates the variation of the average modulus of elasticity at different stress amplitude values with the number of dry-wet cycles. It is evident that during the dry-wet cycles, the average modulus of the samples gradually decreases with an increasing number of

Table 1. Elastic modulus of red sandstone with different stress amplitudes after undergone different dry-wet cycles.

Mechanical parameters	Stress amplitude [MPa]	Dry and wet cycles [N]		
		0	5	10
Modulus of elasticity [GPa]	5–10	9.50	5.34	4.83
	5–15	10.26	6.75	5.76
	5–20	10.89	7.69	6.90
	5–25	11.35	8.17	7.76
	5-30	11.60	8.57	8.19
	5–35	11.98	9.31	8.64
	5–40	12.12	9.93	9.01
	5–45	12.23	10.72	9.42

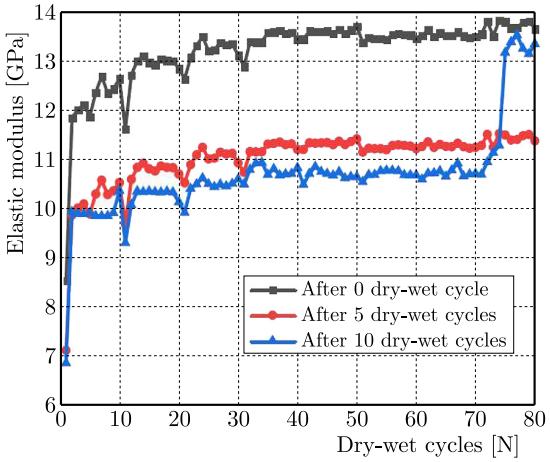

Fig. 9. Elastic modulus of red sandstone after different dry-wet cycle.

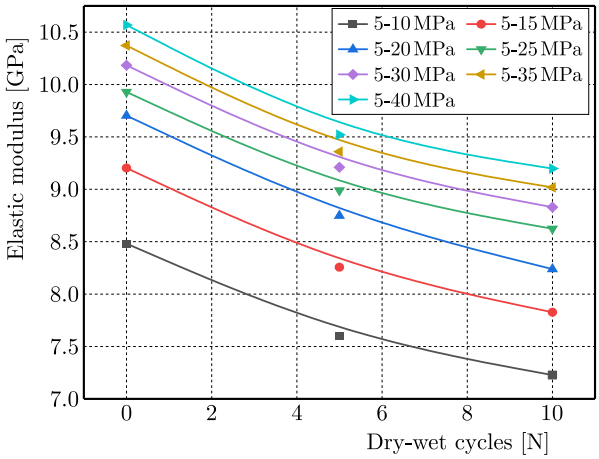

Fig. 10. Curve of elastic modulus vs dry-wet cycle under different cyclic loading.

cycles, a trend that can be expressed using a secondary function. Samples subjected to 5 dry-wet cycles experienced an average decrease in modulus from 42.37 % to 27.56 % compared to samples not subjected to dry-wet cycles. In summary, the initial five dry-wet cycles had the most significant effect on the average elastic modulus of red sandstone samples, closely mirroring the degradation of sample mass during various dry-wet cycles.

Figure 11 shows that the average elastic modulus of red sandstone samples increases with stress amplitude values. However, the growth rate exhibits a gradual slowing trend. The increase in average elastic modulus is most significant at lower stress amplitudes due to the gradual closure of internal cracks under relatively lower stress amplitudes, resulting in a greater increase in stiffness and elastic modulus. As the cyclic stress amplitude value increases, cyclic loading gradually initiates fatigue damage to the samples, leading to the formation of numerous new cracks. Consequently, the stiffness of the rock decreases gradually, and the growth rate of the elastic modulus slows down progressively. The elastic modulus of red sandstone exhibited a significant increase (25.72 % to 76.31 %) when the stress amplitude was elevated from 5 MPa to 40 MPa. This increase was more pronounced at relatively low stress amplitudes (0 MPa to 5 MPa), and the rate of increase slowed as the stress amplitude reached 5 MPa to 30 MPa.

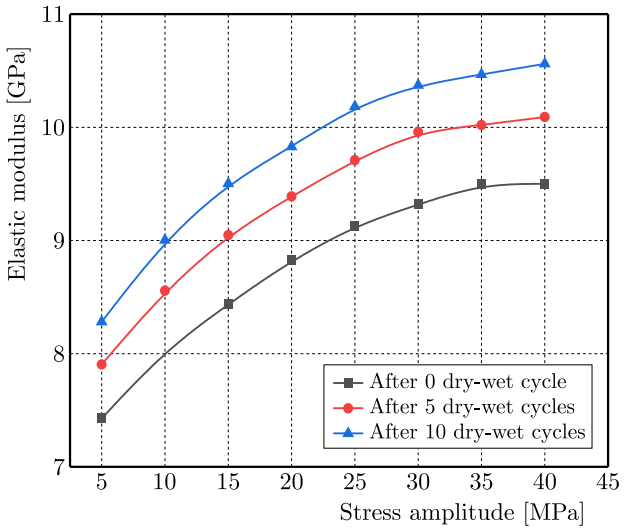

Fig. 11. Curve of elastic modulus vs stress amplitude.

3.5. Failure mode analysis of red sandstone

Figure 12 illustrates the failure modes of sandstone samples subjected to cyclic loading and unloading after a series of dry and wet cycles.

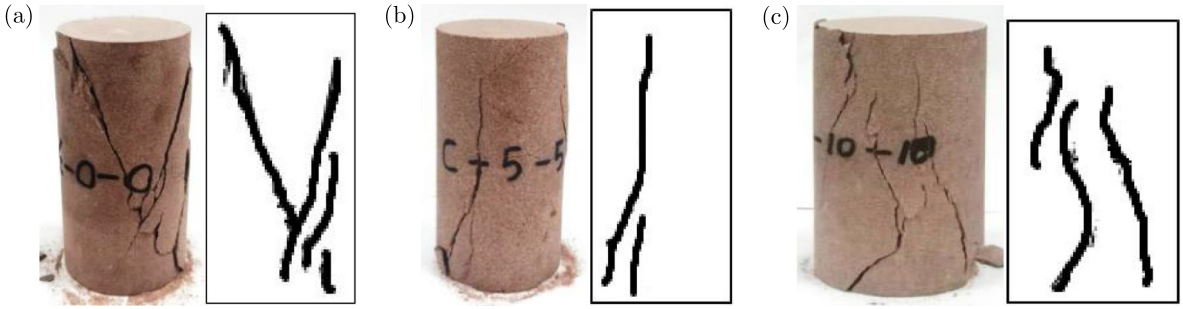

Fig. 12. Uniaxial cyclic load failure mode of red sandstone after different dry-wet cycles: (a) 0 dry-wet cycle; (b) 5 dry-wet cycles; (c) 10 dry-wet cycles.

Figure 12 shows that the failure mode under uniaxial cyclic loading and unloading was primarily splitting failure accompanied by shear failure, differing from the failure modes observed in uniaxial compression tests. The failure mode of red sandstone was predominantly splitting failure throughout the entire specimen. It was also observed that the degree of splitting was greater under cyclic loading due to a significant increase in micro-fractures, volume expansion, and local fractures. This phenomenon becomes increasingly apparent as the number of dry-wet

cycles increases. Additionally, Fig. 12 shows that as the number of dry-wet cycles increases, rock samples become more fragmented, and the number of macro-fractures also rises. Furthermore, as the number of dry-wet cycles increases, the number of through-cracks rapidly escalates.

4. Energy dissipation characteristics

External work is the primary factor contributing to rock failure during rock mechanics experiments (Zhao *et al.*, 2023). Throughout the loading and unloading phases, it is assumed that no heat exchange occurs between the rock sample and its surrounding environment. According to the first law of thermodynamics, the work done by external forces constitutes the total input energy, and the individual energy components can be expressed as

$$U_i = U_{ei} + U_{di}, \tag{4.1}$$

where U_i is the input energy of the i-th cycle, U_{ei} is the elastic energy of the i-th cycle, U_{di} is the dissipated energy of the i-th cycle.

Figure 13 illustrates the schematic diagram of energy calculation under cyclic loading and unloading conditions. The input energy, elastic energy, and dissipated energy of the i-th cycle can be obtained by integrating the loading and unloading sections of the stress-axial strain curve, respectively, as depicted in Eqs. (4.2)–(4.4) (Zhao *et al.*, 2023):

$$U_i = \int_{\varepsilon^l_{\min(2)}}^{\varepsilon^l_{\max}} \mathrm{d}\varepsilon \int_{\sigma_{\min}}^{\sigma_{\max}} f(\sigma_1)\,\mathrm{d}\sigma, \tag{4.2}$$

$$U_{ei} = \int_{\varepsilon^l_{\min(1)}}^{\varepsilon^l_{\max}} \mathrm{d}\varepsilon \int_{\sigma_{\min}}^{\sigma_{\max}} f(\sigma_2)\,\mathrm{d}\sigma, \tag{4.3}$$

$$U_{di} = U_i - U_{ei}, \tag{4.4}$$

where $\sigma_{\max}$ and $\sigma_{\min}$ are the maximum and minimum loading stress, $f(\sigma 1)$ is the equation of loading curve of the i-th cycle, $f(\sigma 2)$ is the equation of unloading curve of the i-th cycle, $\varepsilon^l_{\max}$, $\varepsilon^l_{\min(1)}$, and $\varepsilon^l_{\min(2)}$ are the axial strains at different loading and unloading points of the i-th cycle, respectively.

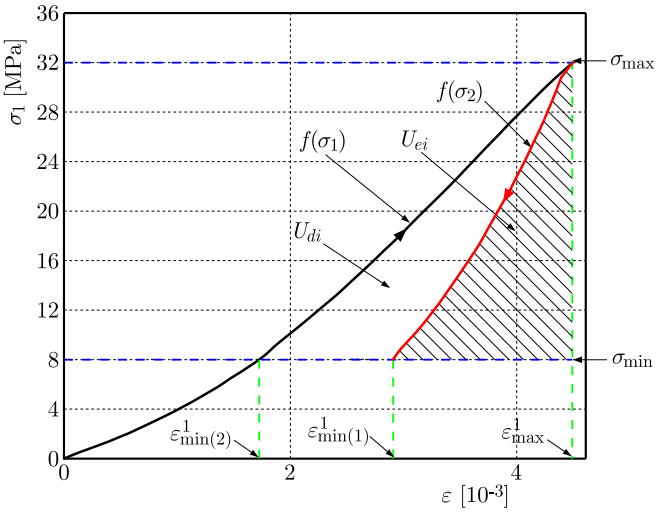

Fig. 13. Schematic diagram of sandstone energy calculation under cyclic loading and unloading condition.

The dissipated energy of sandstone under different loading and unloading after various dry-wet cycles is shown in Fig. 14. It can be observed that dissipated energy increases in stages with rising stress amplitudes. Figure 15 illustrates the variation in dissipated energy between dry-wet cycles under different loading cycles, while Fig. 16 depicts the correlation between dissipated energy and stress amplitudes. It is evident from Fig. 15 that dissipated energy increases logarithmically with the increasing number of dry-wet cycles. From the 0th cycle to the 10th cycle, the dissipated energy under stress amplitudes of 5 MPa, 10 MPa, 15 MPa, 20 MPa, 25 MPa, 30 MPa, 35 MPa, and 40 MPa increased by 138.21 %, 101.48 %, 91.74 %, 83.86 %, 78.90 %, and 65.78 %, respectively. This indicates that the dissipated energy release by the samples accelerates most significantly after five dry-wet cycles. As the number of dry-wet cycles continues to increase, the growth of dissipated energy gradually stabilizes. Throughout the entire process of cyclic loading and unloading of red sandstone, the force applied by the testing machine induces strain, comprising both elastic and plastic strains. The plastic strain escalates with an increasing number of cycles, leading to irreversible permanent deformation of the sample. During cyclic loading, the testing machine causes irreversible damage to the sample, with damage accumulating internally until the rock is ultimately destroyed. From energy Eqs. (4.1)–(4.4), it is evident that the dissipated energy in red sandstone is directly proportional to stress amplitude. As the stress amplitude increases, the dissipated energy also increases. In other words, the energy required

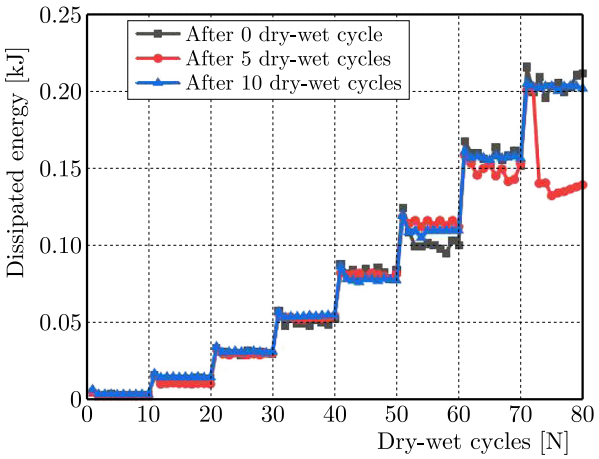

Fig. 14. Curve of the dissipated energy vs loading cycles.

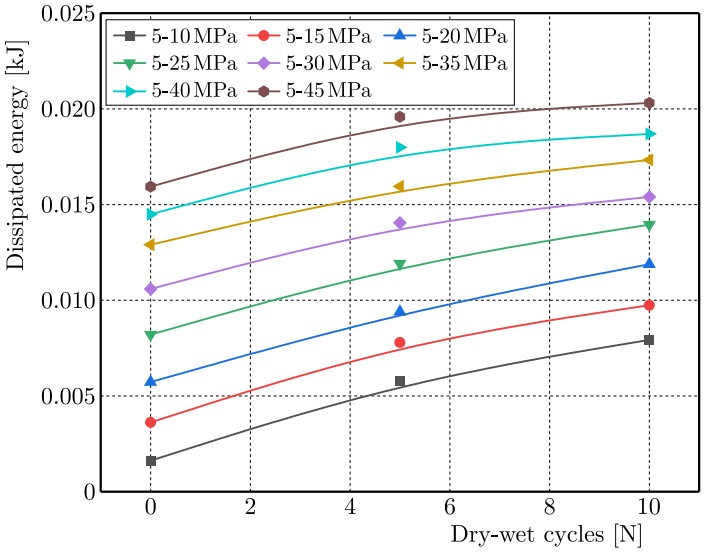

Fig. 15. Curve of the dissipated energy vs dry-wet cycles under different loading cycles.

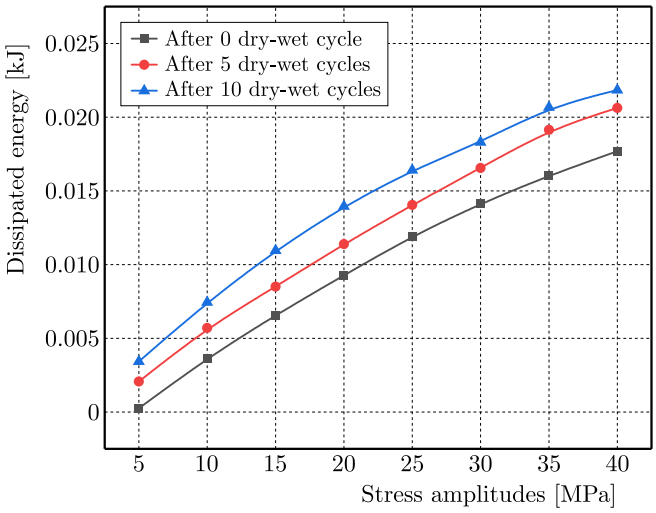

Fig. 16. Curve of the dissipated energy vs stress amplitudes.

to connect the pores and cracks in the rock increases, leading to faster damage and failure, ultimately resulting in a shorter fatigue life of the rock.

Figure 16 illustrates the variation in the dissipated energy law with stress amplitudes at different stress amplitude levels. It can be clearly observed that the dissipated energy of the red sandstone increased with the rise in stress amplitudes. It was found that the dissipated energy increased slowly with stress amplitudes, and a higher number of dry-wet cycles leads to relatively higher dissipated energy under the same stress amplitudes.

5. Conclusion

This research paper assesses the cyclic loading mechanical features and failure patterns of red sandstone after exposure to wet dry-wet cycles. The study aimed to evaluate the degradation of strength parameters, such as peak strength and elastic modulus. Additionally, the energy dissipation characteristics of the samples under cyclic loading were examined, yielding the following primary findings:

The initial 5 dry-wet cycles had a remarkable impact on the sandstone's physical and mechanical properties. The sandstone's mass decreased by 1.16 % after five cycles, and the average elastic modulus of samples under cyclic loads with different stress amplitudes dropped from 42.37 % to 27.56 %, showing that these initial cycles significantly affected the mass and elastic modulus, paralleling the degradation trend during dry-wet cycling.

As the number of dry-wet cycles increased, the stress-strain curve of red sandstone changed notably. The peak stress of samples was substantially reduced under different loading amplitudes, decreasing by 8.31 % after five cycles and 12.88 % after ten cycles. Meanwhile, the primary failure mode of specimens was splitting damage accompanied by partial shear damage.

The dissipated energy demonstrated a clear growth pattern. It increased in stages with the rise of stress amplitudes and logarithmically with the number of dry-wet cycles. From the 0th to the 10th cycle, under stress amplitudes ranging from 5 MPa to 40 MPa, the dissipated energy registered increases between 65.78 % and 138.21 %.

These findings are of paramount importance in comprehending the alterations in the mechanical properties and failure patterns of red sandstone as it undergoes cyclic loading and unloading processes after being subjected to various dry-wet cycles. This understanding provides theoretical guidance for the protection of hazardous slopes in the drawdown zone of the Three Gorges Reservoir.

Acknowledgments

The authors would like to thank the editors and anonymous referees for detailed and valuable suggestions that helped to improve the original manuscript to its present form.

This research was funded by the National Natural Science Foundation of China (grant no. 41302223), the Scientific and Technological Research Program of Chongqing Municipal Education Commission (grant no. KJZD-K2021 01505).

References

1. Akcanca, F. & Aytekin, M. (2014). Impact of wetting-drying cycles on the hydraulic conductivity of liners made of lime-stabilized sand-bentonite mixtures for sanitary landfills. *Environmental Earth Sciences*, *72*(1), 59–66. https://doi.org/10.1007/s12665-013-2936-4
2. Cao, Y.P., Sun, Q., Yang, X.Y., Dang, C., & Geng, J.S. (2022). Sandstone weathering under dry-wet cycling in NaCl solution. *Bulletin of Engineering Geology and the Environment*, *81*(11), Article 490. https://doi.org/10.1007/s10064-022-02992-6
3. Chen, C., Zhao, B.Y., Zhang, L.Y., & Huang, W. (2023). Mechanism of strength deterioration of red sandstone on reservoir bank slopes under the action of dry-wet cycles. *Scientifc Reports*, *13*, Article 20027. https://doi.org/10.1038/s41598-023-47397-x
4. Chen, X.X., He, P., & Qin, Z. (2019). Strength weakening and energy mechanism of rocks subjected to wet-dry cycles. *Geotechnical and Geological Engineering*, *37*(5), 3915–3923. https://doi.org/10.1007/s10706-019-00881-6
5. Fairhurst, C.E. & Hudson, J.A. (1999). Discussion: Draft ISRM suggested method for the complete stress-strain curve for intact rock in uniaxial compression. *International Journal of Rock Mechanics and Mining Sciences*, *36*(3), 279–289. https://doi.org/10.1016/S0148-9062(99)00006-6
6. Gao, D.Y., Sang, S.X., Liu, S.Q., Wu, J., Geng, J.S., Tao, W., & Sun, T.M. (2022). Experimental study on the deformation behaviour, energy evolution law and failure mechanism of tectonic coal subjected to cyclic loads. *International Journal of Mining Science and Technology*, *32*(6), 1301–1313. https://doi.org/10.1016/j.ijmst.2022.10.004
7. Hu, X., Sun, Q., Wang, S.F., Wei, S.N., Ding, X.Y., & Zhao, X.C. (2022). Study on deterioration characteristics of combustion metamorphic rocks under dry-wet cycling. *Bulletin of Engineering Geology and the Environment*, *81*(11), Article 467. https://doi.org/10.1007/s10064-022-02966-8
8. Huan, M., Jiang, S., Zhang, Y.C., Jiang, Y.J., Zhang, X.D., & Xu, C.S. (2024). A new stability analysis model for wet-dry sensitive rocks surrounding underground excavations based on disturbed state concept theory. *International Journal of Rock Mechanics and Mining Sciences*, *174*, Article 105653. https://doi.org/10.1016/j.ijrmms.2024.105653
9. Huang, Z., Zhang, W., Zhang, H., Zhang, J.B., & Zhao, J.H. (2022). Damage characteristics and new constitutive model of sandstone under wet-dry cycles. *Journal of Mountain Science*, *19*(7), 2111–2125. https://doi.org/10.1007/s11629-021-7239-8
10. Li, H., Zhao, B., Hou, Z., & Min, H. (2024). Experimental study on the mechanical properties of rock–concrete composite specimens under cyclic loading. *Buildings*, *14*(3), Article 854. https://doi.org/10.3390/buildings14030854
11. Li, Y.Q., Huang, D., & He, J. (2023). Energy evolution and damage constitutive model of anchored jointed rock masses under static and fatigue loads. *International Journal of Fatigue*, *167*(Part A), Article 107313. https://doi.org/10.1016/j.ijfatigue.2022.107313
12. Liu, S., Yang, G.S., & Dong, X.H. (2019). Experimental study on influence of wetting-drying cycles on mechanical characteristics and damage of red sandstone (in Chinese), *Coal Science and Technology*, *47*(4), 101–106.
13. Liu, X.X., Li, Y., & Wang, W.W. (2022). Study on mechanical properties and energy characteristics of carbonaceous shale with different fissure angles under dry-wet cycles. *Bulletin of Engineering Geology and the Environment*, *81*(8), Article 319. https://doi.org/10.1007/s10064-022-02823-8

14. Ma, D.H., Yao, H.Y., Xiong, J., Zhu, D.Y., & Lu, J.G. (2022). Experimental study on the deterioration mechanism of sandstone under the condition of wet-dry cycles. *KSCE Journal of Civil Engineering*, *26*(6), 2685–2694. https://doi.org/10.1007/s12205-022-1723-8

15. Ministry of Natural Resources, China. (2015). *Regulation for testing the physical and mechanical properties of rock – Part 19: Test for determining the deformability of rock in uniaxial compression* (DZ/T 0276.19-2015).

16. Wang, G.L., Zhang, T.Y., & Zhang, L. (2023). The law of strength damage and deterioration of jointed sandstone after dry-wet cycles. *Journal of Mountain Science*, *20*(4), 1170–1182. https://doi.org/10.1007/s11629-022-7605-1

17. Wang, Y., Feng, W.K., Hu, R.L., & Li, C.H. (2021). Fracture evolution and energy characteristics during marble failure under triaxial fatigue cyclic and confining pressure unloading (FC-CPU) conditions. *Rock Mechanics and Rock Engineering*, *54*(2), 799–818. https://doi.org/10.1007/s00603-020-02299-6

18. Zhao, B.Y., Li, Y.F., Huang, W., Yang, J.S., Sun, J.C., Li, W.C., Zhang, L.Y., & Zhang, L. (2021). Mechanical characteristics of red sandstone under cyclic wetting and drying. *Environmental Earth Sciences*, *80*(22), Article 738. https://doi.org/10.1007/s12665-021-10067-0

19. Zhao, B.Y., Wu, Y.J., Yang, J.S., Sun, J.C., Huang, W., Li, Z.Y., & Zhang, S.H. (2023). Mechanical properties of gas storage sandstone under uniaxial cyclic loading and unloading condition. *Periodica Polytechnica Civil Engineering*, *67*(2), 603–618. https://doi.org/10.3311/PPci.21620

20. Zhao, K., Zhang, L., Yang, D.X., Jin, J.F., Zheng, P., Wang, X., Ran, S.H., & Deng, D.M. (2024). Cyclic impact damage and water saturation effects on mechanical properties and Kaiser effect of red sandstone under uniaxial cyclic loading and unloading compression. *Rock Mechanics and Rock Engineering*, *57*(1), 181–195. https://doi.org/10.1007/s00603-023-03574-y

21. Zhao, Z.H., Yang, J., Zhou, D., & Chen, Y.F. (2017). Experimental investigation on the wetting-induced weakening of sandstone joints. *Engineering Geology*, *225*, 61–67. https://doi.org/10.1016/j.enggeo.2017.04.008

22. Zheng, J.C., Chen, W., Zheng, K.R., Gu, Y.P., Wang, F., Huang, Z., & Li, Y. (2023). Stability analysis of gravity anchor foundation of layered argillaceous sandstone under dry-wet cycles. *Journal of Mountain Science*, *20*(4), 1118–1130. https://doi.org/10.1007/s11629-022-7610-4

23. Zhou, Y., Zhao, D.J., Li, B., Wang, H.Y., Tang, Q.Q., & Zhang, Z.Z. (2021). Fatigue damage mechanism and deformation behaviour of granite under ultrahigh-frequency cyclic loading conditions. *Rock Mechanics and Rock Engineering*, *54*(9), 4723–4739. https://doi.org/10.1007/s00603-021-02524-w

24. Zhou, Y.Q., Sheng, Q., Fu, X.D., & Ding, H.F. (2023). The difference between the dynamic deformation properties of rock material under seismic load and cyclic loading: a case study on Kobe wave. *Mechanics of Time-Dependent Materials*, *27*(2), 401–426. https://doi.org/10.1007/s11043-022-09585-6

Manuscript received October 14, 2024; accepted for publication March 31, 2025; published online April 22, 2025.